


RESEARCH

Open Access



Forebrain-specific conditional calcineurin deficiency induces dentate gyrus immaturity and hyper-dopaminergic signaling in mice

Hideo Hagihara¹, Hiroataka Shoji¹, Mahomi Kuroiwa², Isabella A. Graef³, Gerald R. Crabtree³, Akinori Nishi² and Tsuyoshi Miyakawa^{1*} 

Abstract

Calcineurin (Cn), a phosphatase important for synaptic plasticity and neuronal development, has been implicated in the etiology and pathophysiology of neuropsychiatric disorders, including schizophrenia, intellectual disability, autism spectrum disorders, epilepsy, and Alzheimer's disease. Forebrain-specific conditional Cn knockout mice have been known to exhibit multiple behavioral phenotypes related to these disorders. In this study, we investigated whether Cn mutant mice show pseudo-immaturity of the dentate gyrus (iDG) in the hippocampus, which we have proposed as an endophenotype shared by these disorders. Expression of calbindin and GluA1, typical markers for mature DG granule cells (GCs), was decreased and that of doublecortin, calretinin, phospho-CREB, and dopamine D1 receptor (Drd1), markers for immature GC, was increased in Cn mutants. Phosphorylation of cAMP-dependent protein kinase (PKA) substrates (GluA1, ERK2, DARPP-32, PDE4) was increased and showed higher sensitivity to SKF81297, a Drd1-like agonist, in Cn mutants than in controls. While cAMP/PKA signaling is increased in the iDG of Cn mutants, chronic treatment with rolipram, a selective PDE4 inhibitor that increases intracellular cAMP, ameliorated the iDG phenotype significantly and nesting behavior deficits with nominal significance. Chronic rolipram administration also decreased the phosphorylation of CREB, but not the other four PKA substrates examined, in Cn mutants. These results suggest that Cn deficiency induces pseudo-immaturity of GCs and that cAMP signaling increases to compensate for this maturation abnormality. This study further supports the idea that iDG is an endophenotype shared by certain neuropsychiatric disorders.

Keywords: Calcineurin, Immature dentate gyrus, Dopamine receptor, cAMP, Intellectual disability, Mouse model

Introduction

Endophenotype-oriented neuropsychiatric research has been increasingly considered important to improve the validity, reliability, and translatability of studies from animal models to human disease [1]. Accumulating evidence has indicated that pseudo-immaturity of the hippocampal dentate gyrus (DG) is found in a variety of animal models

that exhibit behavioral abnormalities related to schizophrenia, intellectual disability (ID), autism spectrum disorders (ASD), epilepsy, and Alzheimer's disease (AD) [2–13]. In the immature DG (iDG) phenotype, molecular expression patterns in the DG of adult mice resemble those of typically developing infants or adolescents with reduced mature marker (e.g., calbindin, glutamate receptor 1 [GluA1]) and increased immature marker (e.g., calretinin, doublecortin) expression. Importantly, pseudo-immaturity phenomena in the DG and other brain regions have been identified in human patients with schizophrenia, ASD, epilepsy, and AD, as assessed

*Correspondence: miyakawa@fujita-hu.ac.jp

¹ Division of Systems Medical Science, Center for Medical Science, Fujita Health University, Toyoake, Aichi 470-1192, Japan
Full list of author information is available at the end of the article



© The Author(s) 2022. **Open Access** This article is licensed under a Creative Commons Attribution 4.0 International License, which permits use, sharing, adaptation, distribution and reproduction in any medium or format, as long as you give appropriate credit to the original author(s) and the source, provide a link to the Creative Commons licence, and indicate if changes were made. The images or other third party material in this article are included in the article's Creative Commons licence, unless indicated otherwise in a credit line to the material. If material is not included in the article's Creative Commons licence and your intended use is not permitted by statutory regulation or exceeds the permitted use, you will need to obtain permission directly from the copyright holder. To view a copy of this licence, visit <http://creativecommons.org/licenses/by/4.0/>. The Creative Commons Public Domain Dedication waiver (<http://creativecommons.org/publicdomain/zero/1.0/>) applies to the data made available in this article, unless otherwise stated in a credit line to the data.

by decreased calbindin expression and/or increased calcineurin expression and genome-wide gene expression patterns in post-mortem brain tissues [14–20], suggesting that pseudo-immaturity of particular brain regions is a phenomenon that can be observed across species. We have proposed iDG as a brain endophenotype shared by certain types of neuropsychiatric disorders [21].

Calcineurin (Cn) is a heterodimeric calcium/calmodulin-dependent serine/threonine protein phosphatase comprising Cnb regulatory and Cna catalytic subunits [22]. Cnb1, an isoform of Cnb, is the only regulatory subunit expressed in the brain, while several different Cna isoforms are expressed in the brain [22], with a particular abundance in the hippocampus, cortex, and striatum [23, 24]. Cn is known to be involved in a wide range of neuronal functions and development, such as *N*-methyl-D-aspartate (NMDA) receptor-dependent long-term depression in hippocampal CA1 neurons [25, 26], dendritic spine size dynamics in cortical neurons [26, 27], and axonal outgrowth in some types of embryonic neurons [29, 30]. Genetic studies have suggested an association between the genes encoding CNA isoforms and schizophrenia [31–34]. Recently, de novo mutations in *PPP3CA*, a gene encoding a CNA isoform, have been repeatedly reported as a cause of ID /developmental delay and epilepsy, which are often accompanied by autistic features [35–40]. More recent large-scale association studies have identified a number of genes that have common and rare variants associated with schizophrenia [41–43] and showed a nominal association for rare variants in *PPP3CA* with no genome-wide significance [41]. RNA sequencing analysis has revealed that expression of *CNB1* (*PPP3R1*) is reduced in the cortex of patients with ASD [44]. Mutant mice with forebrain neuron-specific deletion of *Cnb1* (Cn mutants) exhibited multiple behavioral abnormalities related to schizophrenia and other neuropsychiatric disorders, including hyper-locomotor activity (mania-like behavior), reduced nest-building activity (a mimic of negative-like symptoms [45]), and working memory deficits [24, 46], supporting the idea that alterations in CN signaling or in mechanism(s) supported by CN functions may be an important contributing factor in the pathogenesis of these diseases [46]. However, it remains unknown whether Cn deficiency causes neuronal pseudo-immaturity in the DG, and if so, what behaviors are associated with such an immature phenotype. In addition, it is unknown whether Cn mutants exhibit increased expression of *Drd1*, a shared feature among mouse models with the iDG phenotype [21], such as *Camk2a*[±] mice and the mice chronically treated with the antidepressant fluoxetine [47, 48]. An increase in *DRD1* expression has been observed in some cortical regions of patients with schizophrenia [49–51].

The current study addresses these questions using molecular expression pattern analyses, phosphorylation assays of *Drd1* signaling substrates, and behavioral tests in combination with pharmacological manipulation to rescue the observed multi-level phenotypes in Cn mutant mice.

Methods

A detailed description of the Materials and Methods is provided in the Additional file 1: Supplementary Materials and Methods.

Animals

All animal experiments were approved by the Institutional Animal Care and Use Committee of Fujita Health University and Kurume University based on the Law for the Humane Treatment and Management of Animals and the Standards Relating to the Care and Management of Laboratory Animals and Relief of Pain. Every effort was made to minimize the number of animals used. The forebrain-specific *Cnb* deficient mice were generated by mating a male mouse homozygous for floxed *Cnb* (*Cnb*^{flox/flox}) [52] with a female *Cnb*^{flox/wild} mouse carrying the calcium/calmodulin-dependent protein kinase II alpha-Cre transgene (*Camk2a-Cre*[±]) [53]. *CNB* floxed mice and *Camk2a-Cre* mice were backcrossed to C57BL6/J mice for at least seven and ten generations, respectively, before experimental intercrosses. The resulting genotypes were *Camk2a-Cre*^{-/-}, *Cnb*^{flox/wild}; *Camk2a-Cre*[±], *Cnb*^{flox/wild}; *Camk2a-Cre*^{-/-}, *Cnb*^{flox/flox}; and *Camk2a-Cre*[±], *Cnb*^{flox/flox}. We confirmed that the first three genotypes showed no significant difference in expression of mature/immature granule cell markers (Additional file 1: Fig. S1). Therefore, *Camk2a-Cre*^{-/-}, *Cnb*^{flox/wild} mice, *Camk2a-Cre*[±], *Cnb*^{flox/wild} mice, or *Camk2a-Cre*^{-/-}, *Cnb*^{flox/flox} mice were used for the littermate control group and *Camk2a-Cre*[±], *Cnb*^{flox/flox} mice were used for the *Cnb* deficient group. We used male and female adult mice (>8 weeks old) in this study.

Immunohistochemistry

Immunohistochemical analysis was performed as previously described [54, 55]. Primary antibodies used in this study are listed in Additional file 2: Table S1. Immunoreactivity to the antigen was visualized using Alexa Fluor 488-conjugated secondary antibody (Molecular Probes, Eugene, OR). Nuclear staining was performed with Hoechst 33,258 (Polysciences, Warrington, PA). We used a microscope (LSM 510 META; Zeiss, Göttingen, Germany) to obtain images of the stained sections. Three to seven sections from each animal were processed for semi-quantification analyses, and the averaged values were considered as one sample. Immunofluorescence intensity and the number of stained cells were counted in

the indicated hippocampal regions, manually delineated using ZEN software (Zeiss) or ImageJ software (<http://rsb.info.nih.gov/ij/>) according to the mouse brain atlas [56]. Semi-quantification analyses were performed in the dorsal hippocampus (approximately from -2.1 to -1.6 mm from the bregma).

Real-time quantitative PCR

We used 11-week-old mice for the analysis [57]. The following primers were used: dopamine d1 receptor (Drd1a) (1–124), 5'-ATGGCTCCTAACACTTCTACCA and 5'-GGGTATTCCCTAAGAGAGTGGAC; tryptophan 2,3-dioxygenase (Tdo2) (1–105), 5'-ATGAGTGGGTGCCCGTTTG and 5'-GGCTCTGTTTACACCAGTTTGGAG; desmoplakin (Dsp) (7–113), 5'-GCTGAAGAACTCTAGCCCA and 5'-ACTGCTGTTTCCTCTGAGACA; and β -actin (851–962), 5'-AGTGTGACGTTGACATCCGTA and 5'-GCCAGAGCAGTAATCTCCTTCT. Ct values used were the means of two or three replicates (Additional file 2: Table S2).

DNA microarray and data processing

Dissection of the mouse DG [57] and microarray experiments were performed as described previously [54]. Thirteen to 14 weeks old Cn mutant and control mice were used. The raw microarray data were deposited in the GEO database under accession number GSE175896, and the processed data is available in Additional file 2: Table S3. The following microarray datasets were also used: the DG of postnatally developing mice (GSE113727) [17, 58], the DG of Camk2a[±] mice [57], the DG of Hivep2 (also called Schnurri-2) knockout (KO) mice (GSE42777) [3], and the DG of mice chronically treated with an antipsychotics fluoxetine (GSE118669) [58].

Using the expression values, we calculated fold changes and t-test P-values between experimental mice and the corresponding control mice. The average value of 8, 11, 14, 17, 21, and 25 days old mice was divided by that of 29 days old mice, respectively. Genes (or transcripts) with absolute fold change >1.2 and P-value <0.05 (without correction for multiple testing) were imported to the web-based bioinformatics tool BaseSpace (Illumina, San Diego, CA; <https://basespace.illumina.com>) [59] according to the manufacturer's instructions. Subsequently, the gene expression patterns of the two given gene sets were statistically compared using BaseSpace [17, 60, 61]. Using the bioinformatics tool, similarities were examined using the Running Fisher algorithm, a nonparametric rank-based statistical method, in which information regarding the rank based on the absolute value of fold change and the direction of gene expression changes within each gene set was considered [59]. The greater the similarity in gene expression patterns between the two conditions, the

lower the resulting overlap P-value. Details of the algorithm have been described previously [3].

Pathway enrichment analysis

Pathways/bigroups enriched in the differentially expressed genes (DEGs) were determined through a combination of rank-based enrichment statistics and biomedical ontologies using BaseSpace [59]. Pathways/bigroups from GO and canonical pathways of Broad MSigDB were included in this analysis.

Drug treatment

Eight-week-old mice were administered with 2 mg/kg of rolipram (R6520; Sigma-Aldrich, St Louis, MO) or vehicle (1% dimethyl sulfoxide in saline) intraperitoneally once daily at a volume of 5 ml/kg for 3 weeks. On the next day of the final treatment, mice were processed for immunohistochemical analyses, slice experiments, and behavioral tests. Mice for behavioral testing were kept treated with rolipram, which was administered at the end of the experiments every day, during behavioral testing.

Slice experiments

Preparation of DG slices and immunoblotting were performed as described previously [48]. Briefly, the regions of DG were dissected from 350- μ m-thick coronal slices between -1.4 and -3.8 mm from the bregma. The DG slices were incubated with or without SKF81297 (Sigma-Aldrich) for 10 min and processed for immunoblotting analysis. Eight mice were analyzed for each condition. Primary antibodies used in this study are listed in Additional file 2: Table S1.

Behavioral tests

The open field test, T-maze test, startle response/pre-pulse inhibition (PPI) test, and nest building test was performed as described previously [3, 46, 62–64].

Statistical analysis

The data were analyzed by Student's t-test, one-way ANOVA, or two-way ANOVA followed by Sidak's multiple comparison test using R or Prism 8 version 8.4.2 (GraphPad Software, Inc., San Diego, CA). We used the nonparametric tests (Mann Whitney test and Friedman test) when the homogeneity of variance and normality assumptions were not met. In the behavioral test battery, we defined "study-wide significance" as the statistical significance that survived false discovery rate (FDR) correction for 14 indices in the comparison between Mut + Rol and Mut + Veh groups and "nominal significance" as the one that achieved a statistical significance in an index ($P < 0.05$) but did not survive this correction.

Results

Cn deficiency induces immature dentate gyrus phenotype as assessed by typical neuronal maturation markers

We first examined the expression patterns of typical markers of mature and immature GCs in the DG. The immunoreactive intensity of calbindin, a mature GC marker, was drastically decreased in the GC layer of Cn mutants (Fig. 1a). The number of calbindin-positive cells was also decreased in the GC layer of Cn mutants (Con, 4078.8 ± 172.6 cells/mm²; Mut, 1285.2 ± 341.0 cells/mm²; $P < 0.0001$). Immunoreactive intensity of GluA1 and GluA2, other markers of mature GC [65], was decreased in the GC layer (Fig. 1b and c) and molecular layer (Additional file 1: Fig. S2) of Cn mutants, indicating the reduced expression of GluA1 and GluA2 in both soma and dendrites of GC. The number of Hoechst-stained nuclei in the GC layer was not significantly different between genotypes (mutants: 112.64 ± 3.59 cells/mm², controls: 113.43 ± 5.10 cells/mm²; $P = 0.90$), indicating that the decreased expression of those mature GC markers in Cn mutants was not due to the loss of GCs. Expression levels of mRNA for other mature GC markers, *Dsp* and *Tdo2* [66], were also significantly lower in the DG of Cn mutants (Fig. 1i). In contrast, the expression of doublecortin (Fig. 1d), PSA-NCAM (Fig. 1e), and calretinin (Fig. 1f), markers for progenitors or immature GCs, was higher in the Cn mutants. Doublecortin-positive cells were observed within the GC layer in Cn mutants, whereas in controls, such cells were mostly located in the subgranular zone, where GCs proliferate and differentiate into new neurons (Fig. 3d). We also found that the expression of phospho-cAMP-dependent response element binding protein (CREB), which is predominantly expressed in immature GCs and located in the inner GC layer in the normal adult DG [67–69], was increased throughout the GC layer in Cn mutants (Fig. 1g), while the expression levels of total CREB were almost normal (Fig. 1h). Western blot analysis confirmed increased CREB phosphorylation in the DG of Cn mutants (Fig. 1i, Additional file 1: Fig. S3).

We also found that the expression of *Drd1a* mRNA was increased in the DG of Cn mutants compared to that in controls (Fig. 1j).

An additional feature common to iDG mouse models is the activation of astrocytes in the DG [21]. Studies in human post-mortem brains have suggested activation of astrocytes in the brain of patients with neuropsychiatric disorders, including ASD [70, 71], ID [72], epilepsy [73, 74], schizophrenia [75, 76], and AD [77], which are considered inflammatory conditions of the brain [75]. In Cn mutants, the expression of glial fibrillary acidic protein (GFAP), an astrocytic marker, increased significantly in the molecular layer of the DG, while the number of GFAP-positive cells was not different from that in controls (Fig. 2a). Moreover, the expression of S100 calcineurin binding protein B (S100B), another marker of astrocytes, was increased significantly in the molecular layer of the DG, while the number of S100B-positive cells was not different from that in controls (Additional file 1: Fig. S4). We found that neither expression of the microglial marker Iba1 nor the number of Iba1-positive cells was changed in Cn mutants (Fig. 2b). These results suggest astrogliosis with no apparent microgliosis in the DG of Cn mutants. Thus, Cn mutants showed the iDG phenotype as assessed by typical marker expressions that were common to previously identified mouse models with iDG [21].

Transcriptomic evidence for the immaturity of the DG in Cn mutant mice

Next, we evaluated the iDG phenotype in Cn mutants at a genome-wide gene expression level. Microarray analysis revealed that of 45,037 transcripts tested, 353 were differentially expressed in the DG of Cn mutants compared to controls (absolute fold change > 1.2 , $P < 0.05$, without correction for multiple tests; Fig. 3a). *Cnbl* (*Ppp3r1*) displayed the lowest value among the differentially expressed genes (DEGs) (Additional file 2: Table S3). Pathway analysis showed that terms related to cell proliferation and development were enriched in the DEGs

(See figure on next page.)

Fig. 1 Immature dentate gyrus phenotype assessed using typical molecular markers in Cn mutant mice. **a–h** Immunostaining images and quantified bar graphs of calbindin (**a**; $t = 11.20$, $df = 22$, $P < 0.0001$), GluA1 (**b**; $t = 16.66$, $df = 22$, $P < 0.0001$), GluA2 (**c**; $t = 10.00$, $df = 4$, $P = 0.0006$), doublecortin (**d**; left graph: $t = 4.39$, $df = 4$, $P = 0.012$; right graph: $t = 11.66$, $df = 826$, $P < 0.0001$), PSA-NCAM (**e**; F test: $P < 0.0001$; Mann Whitney test: $P < 0.0001$), calretinin (**f**; $t = 11.23$, $df = 22$, $P < 0.0001$), phospho-CREB (**g**; F test: $P < 0.0001$; Mann Whitney test: $P = 0.0091$), and CREB (**h**; $t = 0.24$, $df = 10$, $P = 0.81$). **i** Western blot images and quantified bar graphs of phospho-CREB and CREB. Graphs show relative levels of phospho-CREB over total CREB. $P = 0.0085$. The original blots are included in Additional file 1: Fig. S3. **j** Expression levels of *Dsp*, *tdo2*, and *Drd1a* mRNA (*Dsp*: $t = 6.95$, $df = 13$, $P < 0.0001$; *Tdo2*: $t = 10.64$, $df = 14$, $P < 0.0001$; *Drd1a*: $t = 2.71$, $df = 13$, $P = 0.018$). Bar graphs show means \pm SEM. Each dot represents one mouse, except for the right graph in **d**. The positions of doublecortin-positive cells are shown as relative values between the subgranular layer (0) and the border with the molecular layer (1) (**d**, right graph; each dot represents one cell). Scale bars: **a** upper panels 500 μ m, lower panels 50 μ m; **b**, **c** left panels 500 μ m, right panels 100 μ m; **d**, **e** left panels 300 μ m, right panels 50 μ m; **f** left panels 200 μ m, right panels 50 μ m; **g**, **h** 50 μ m. Relative intensity means the ratio of the immunoreactive intensity obtained from the mutants to that of the controls. * $P < 0.05$, ** $P < 0.01$, Students t-test. Con, control mice; Mut, Cn mutant mice

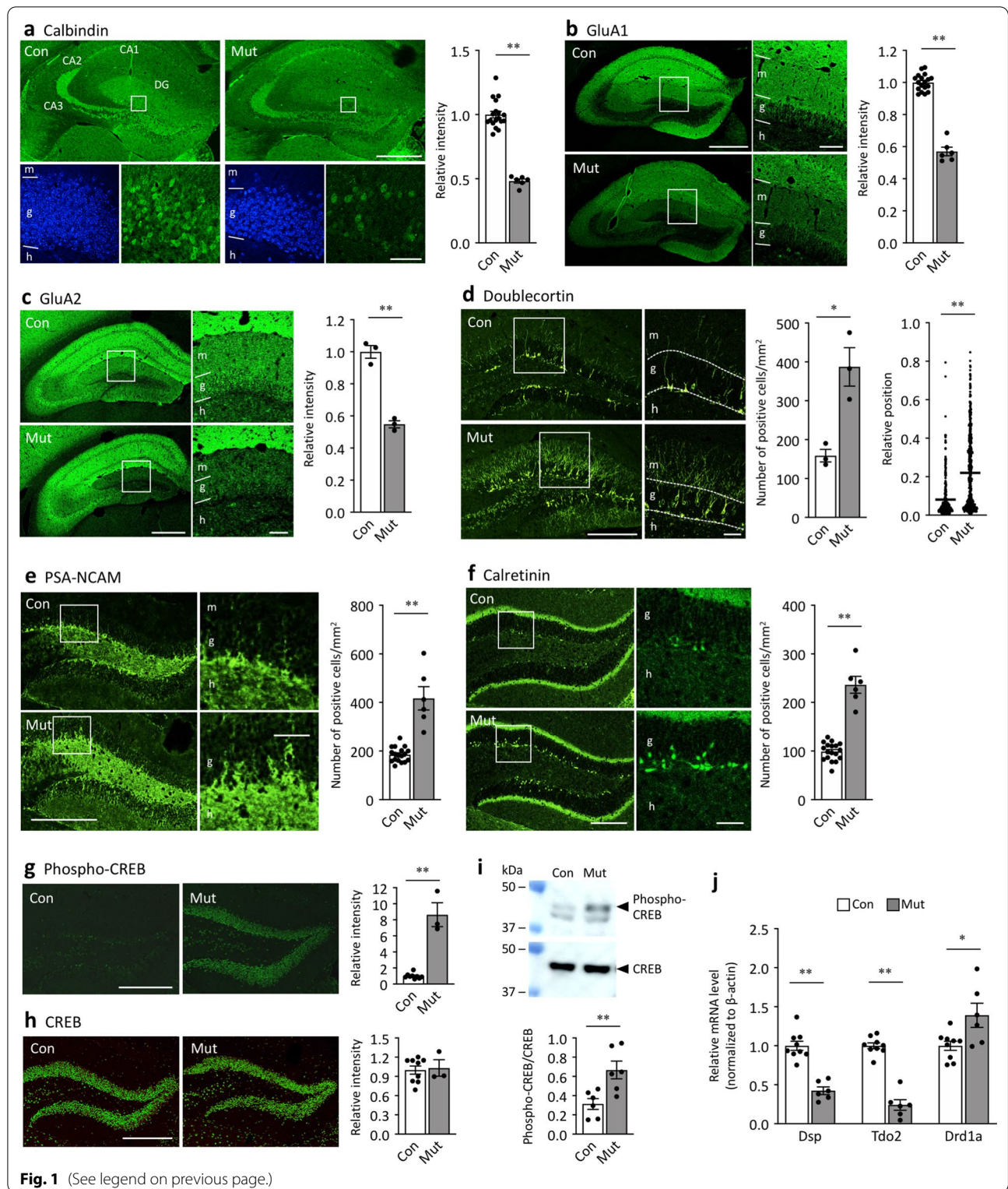
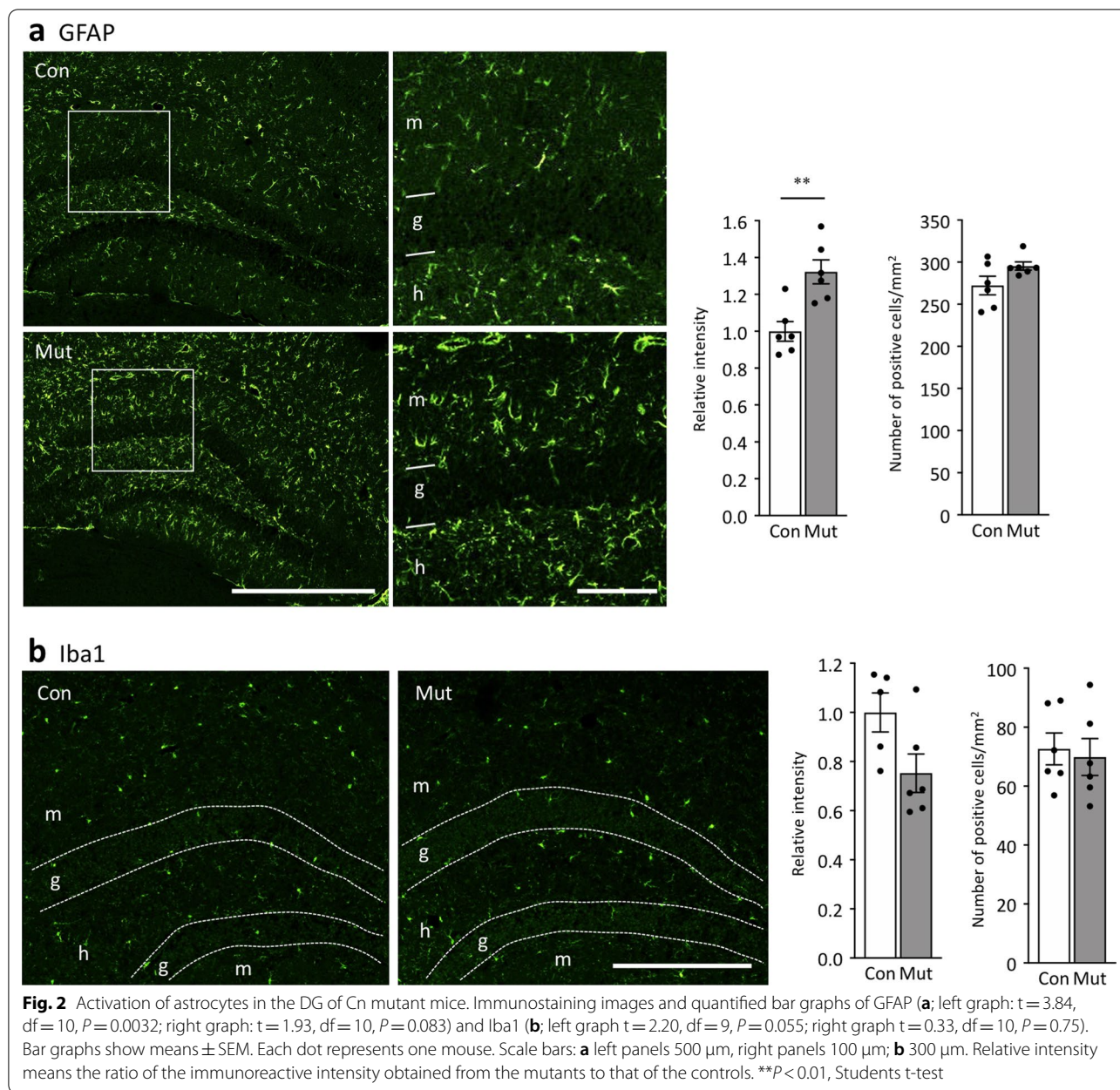


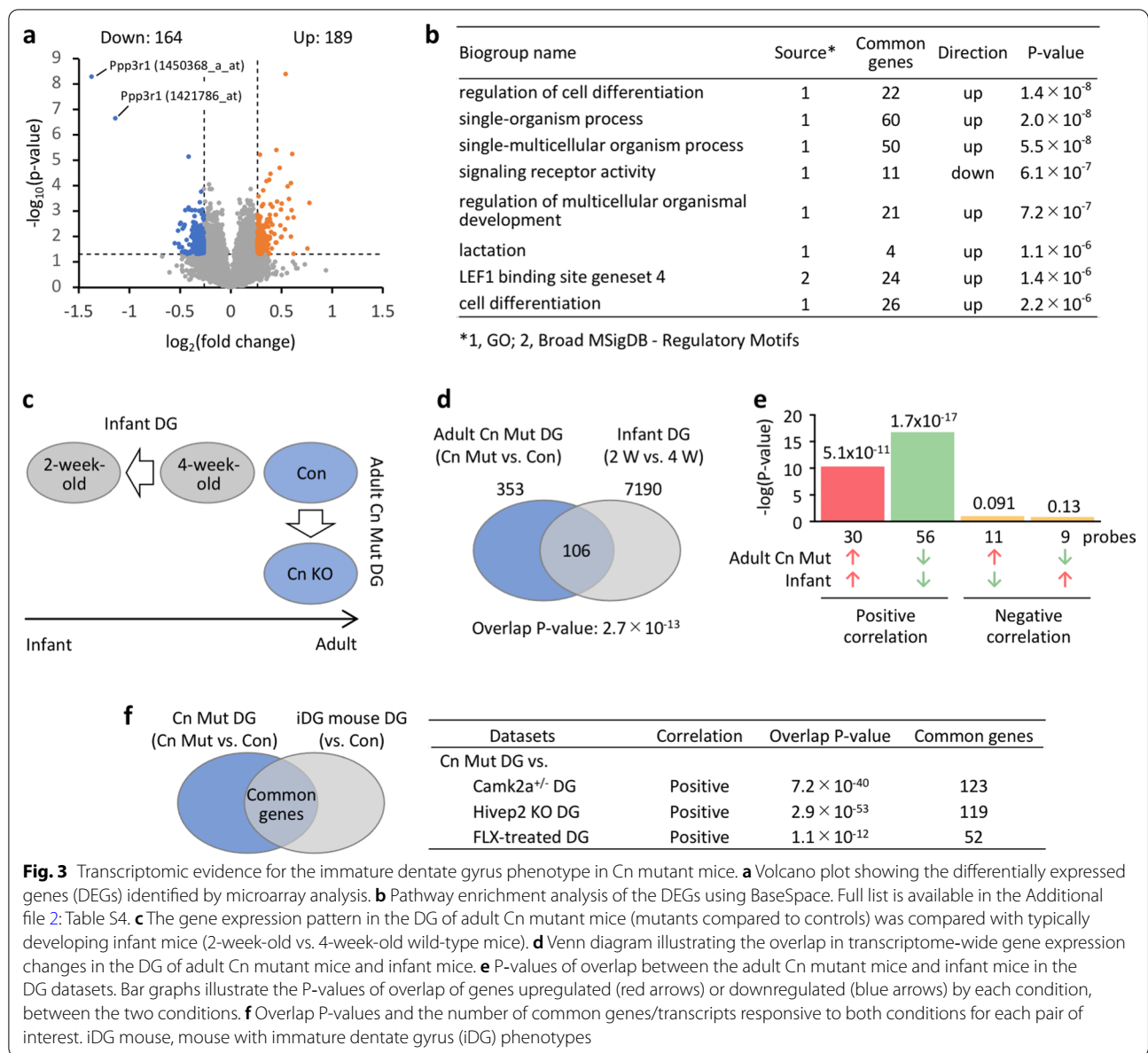
Fig. 1 (See legend on previous page.)



(Fig. 3b; Additional file 2: Table S4), supporting the idea of maturation abnormalities in the DG of Cn mutants.

To further define the iDG phenotype in Cn mutants, we used publicly available microarray datasets to conduct a comparative transcriptomic analysis. This analysis examined whether, or to what extent, overall gene expression patterns were similar between adult Cn mutants and typically developing infant mice (Fig. 3c). Transcriptome datasets were compared using the Running Fisher test, a non-parametric rank-based statistical method, which calculates overlap P-values between two given gene sets in consideration of fold-change-based

rank and the direction of changes [59]. In this analysis, we identified a highly significant overlap P-value with a positive correlation between the DG of adult Cn mutants (mutants vs. controls) and the DG of infant mice (2-week-old vs. 1-month-old) ($P = 2.7 \times 10^{-13}$; Fig. 3d and e, Additional file 2: Table S5), indicating a significant similarity in the gene expression patterns between them. Furthermore, the patterns of gene expression changes in Cn mutants were similar to those in Hivep2 KO mice [3], Camk2a $^{\pm}$ mice [2], and fluoxetine-treated mice [47, 48], and other mouse models with iDG (Fig. 3f). These results confirmed the



iDG phenotype in Cn mutants from a transcriptomic standpoint.

Chronic rolipram treatment ameliorates iDG phenotype and nest-building behavior

Increased expression of *Drd1a*, which stimulates intracellular cAMP signaling, is a common feature found in previously identified mouse models with iDG [20], and an increase was also found in Cn mutants (Fig. 1i). We also found an increase in CREB phosphorylation (Fig. 1g and h), which are known to be increased by cAMP/protein kinase A (PKA) [78], while CREB is

suggested to be not a direct target of Cn [79]. These results suggest that cAMP signaling is elevated in the DG of Cn mutants. We previously found that chronic treatment with rolipram, a cAMP-specific phosphodiesterase inhibitor that elevates intracellular cAMP levels (in combination with ibuprofen), rescued the iDG phenotype in *Hivep2* KO mice [3], raising the possibility that the increased cAMP signaling in Cn mutants is due to a compensatory mechanism. To determine whether the increased cAMP signaling is related to compensatory or pathological mechanisms underlying the iDG and behavioral phenotypes, we investigated the effect of rolipram on the phenotypes of Cn mutants.

The rolipram treatment significantly increased the expression levels of the mature GC marker calbindin ($P=0.0057$; Fig. 4a and b) and decreased the expression levels of the immature GC marker phospho-CREB ($P=0.033$; Fig. 4a and c) in Cn mutants. Expression levels of GluA1 were not affected by rolipram treatment (Additional file 1: Fig. S5), and the number of doublecortin-positive (Fig. 4d) and calretinin-positive cells (Fig. 4e) tended to be lower following rolipram treatment in Cn mutants. These results suggest that chronic treatment with rolipram partially rescued the iDG phenotype in Cn mutants. Moreover, chronic rolipram treatment decreased the expression of the astrocytic marker, GFAP, in mutants ($P=0.010$; Fig. 4f), which may be due to the anti-inflammatory effects of the drug [80].

A series of behavioral tests revealed that chronic rolipram treatment improved the impaired nest-building activity in Cn mutants at a nominal significance level (raw $P=0.025$; Fig. 4g). Chronic treatment with rolipram did not significantly affect locomotor activity or anxiety-like behavior in the open field test (Additional file 1: Figs. S6a–S6d), prepulse inhibition (Additional file 1: Figs. S6e and S6f), or working memory assessed using the T-maze spontaneous alternation task (Additional file 1: Fig. S6g). Thus, rolipram treatment selectively rescued impaired nesting behavior, which is considered to be associated with negative symptoms of psychiatric disorders [45].

Increased Drd1a/PKA signaling activity in the DG of Cn mutant mice

Considering the increased expression of Drd1a in Cn mutants and the cAMP-modulating effect of rolipram, we investigated cAMP-dependent PKA signaling activity downstream of Drd1a to gain mechanistic insights into the rescue effects of rolipram. After the 3-week treatment of mice with rolipram or vehicle, we prepared DG slices and examined the phosphorylation levels of known substrates of PKA (P-Ser845 GluA1, P-Thr34 dopamine- and cAMP-regulated phosphoprotein of 32 kDa [DARPP-32], and P-Ser133 phosphodiesterase 4 [PDE4]) or a downstream substrate of PKA (P-Thr202/Tyr204 extracellular signal-regulated kinase 2 [ERK2]) with or without incubation with SKF81297, a Drd1-like agonist.

In the vehicle-treated group (Fig. 4h–k and Additional file 1: Fig. S7), the effect of genotype on phosphorylation levels of all four substrates for PKA signaling was examined under both basal and SKF81297-stimulated conditions, suggesting that Drd1a-mediated PKA signaling is activated in Cn mutants. Interestingly, in the rolipram-treated group (Fig. 4l–o), phosphorylation levels of P-Ser845 GluA1 and P-Thr202/Tyr204 ERK2 were not significantly different between Cn mutants and controls (Fig. 4l and m), whereas levels of P-Thr34 DARPP-32 and P-Ser133 PDE4 remained increased in Cn mutants (Fig. 4n and o). In Cn mutants, chronic rolipram treatment shifted P-Ser845 GluA1 and P-Thr202/Tyr204 ERK2 levels downward, and there was a tendency of decrease in P-Ser845 GluA1 levels ($P=0.090$ for P-Ser845 GluA1 and $P=0.13$ for P-Thr202/Tyr204 ERK2)

(See figure on next page.)

Fig. 4 Rescue of immature dentate gyrus phenotype and impaired nest building behavior by chronic rolipram treatment in Cn mutant mice. **a** Immunostaining images of calbindin (upper panels) and phospho-CREB (lower panels). Scale bars, 200 μ m. G, granule cell layer; h, hilus. **b–g** Bar graphs showing the number of calbindin-positive cells (**b**; Bartlett test: genotype, $P=0.0037$, drug, $P=0.11$; Friedman test: genotype effect: $F(1, 11)=33.52$, $P<0.0001$; drug effect: $F(1, 11)=13.84$, $P=0.0034$; interaction: $F(1, 11)=9.79$, $P=0.0096$), the number of phospho-CREB-positive cells (**c**; Bartlett test: genotype, $P=0.016$, drug, $P=0.024$; Friedman test: genotype effect: $F(1, 16)=45.15$, $P<0.0001$; drug effect: $F(1, 16)=7.37$, $P=0.015$; interaction: $F(1, 16)=3.59$, $P=0.076$), the number of doublecortin (Dcx)-positive cells (**d**; genotype effect: $F(1, 10)=6.50$, $P=0.029$; drug effect: $F(1, 10)=2.04$, $P=0.18$; interaction: $F(1, 10)=4.22$, $P=0.067$), number of calretinin (CR)-positive cells (**e**; Bartlett test: genotype, $P=0.023$, drug, $P=0.13$; Friedman test: genotype effect: $F(1, 10)=10.81$, $P=0.0082$; drug effect: $F(1, 10)=6.15$, $P=0.033$; interaction: $F(1, 10)=5.22$, $P=0.046$), GFAP immunoreactivity (**f**; Bartlett test: genotype, $P=0.016$, drug, $P=0.024$; Friedman test: genotype effect: $F(1, 11)=33.52$, $P=0.00012$; drug effect: $F(1, 11)=12.14$, $P=0.0051$; interaction: $F(1, 11)=10.23$, $P=0.0085$), and nest-building score (g; genotype effect: $F(1, 55)=17.70$, $P<0.0001$; drug effect: $F(1, 55)=4.45$, $P=0.040$; interaction: $F(1, 55)=3.82$, $P=0.056$). $*P<0.05$, $**P<0.01$, two-way ANOVA or Friedman test followed by multiple comparison test. Bar graphs show means \pm SEM. Each dot represents one mouse. **h–o** Expression levels of P-Ser845 GluA1 (**h, l**), P-Thr202/Tyr204 ERK2 (**i, m**), P-Thr34 DARPP-32 (**j, n**), and P-Ser133 PDE4B1 (**k, o**) in the DG slices from vehicle (Veh)-treated mice (**h–k**) or rolipram (Rol)-treated mice (**l–o**) with or without preincubation with SKF81297. The data were normalized to total protein and values obtained with untreated slices from vehicle-treated control mice. The expression levels of total proteins were not altered significantly between genotypes or in response to SKF81297. The original blots are included in Additional file 1: Fig. S7. $*P<0.05$, $**P<0.01$, two-way ANOVA or Friedman test. **h** Bartlett test: genotype, $P=0.00075$, SKF81297, $P=0.013$; Friedman test: Genotype effect: $F(1, 42)=15.55$, $P=0.00030$; effect of SKF81297: $F(2, 42)=26.14$, $P<0.0001$; interaction: $F(2, 42)=0.45$, $P=0.64$. **i** Genotype effect: $F(1, 42)=23.11$, $P<0.0001$; effect of SKF81297: $F(2, 42)=18.57$, $P<0.0001$; interaction: $F(2, 42)=0.26$, $P=0.77$. **j** Genotype effect: $F(1, 42)=18.35$, $P=0.0001$; effect of SKF81297: $F(2, 42)=12.94$, $P<0.0001$; interaction: $F(2, 42)=0.78$, $P=0.46$. **k** Genotype effect: $F(1, 36)=42.55$, $P<0.0001$; effect of SKF81297: $F(2, 36)=4.07$, $P=0.026$; interaction $F(2, 36)=1.87$, $P=0.17$. **l** Genotype effect: $F(1, 42)=0.015$, $P=0.90$; effect of SKF81297: $F(2, 42)=15.41$, $P<0.0001$; interaction: $F(2, 42)=0.13$, $P=0.88$. **m** Genotype effect: $F(1, 42)=0.14$, $P=0.71$; effect of SKF81297: $F(2, 42)=19.15$, $P<0.0001$; interaction: $F(2, 42)=0.068$, $P=0.93$. **n** Genotype effect: $F(1, 42)=5.09$, $P=0.0293$; effect of SKF81297: $F(2, 42)=12.52$, $P<0.0001$; interaction: $F(2, 42)=0.39$, $P=0.68$. **o** Genotype effect: $F(1, 36)=36.62$, $P<0.0001$; effect of SKF81297: $F(2, 36)=7.04$, $P=0.0026$; interaction: $F(2, 36)=1.34$, $P=0.27$. Data are shown as means \pm SEM

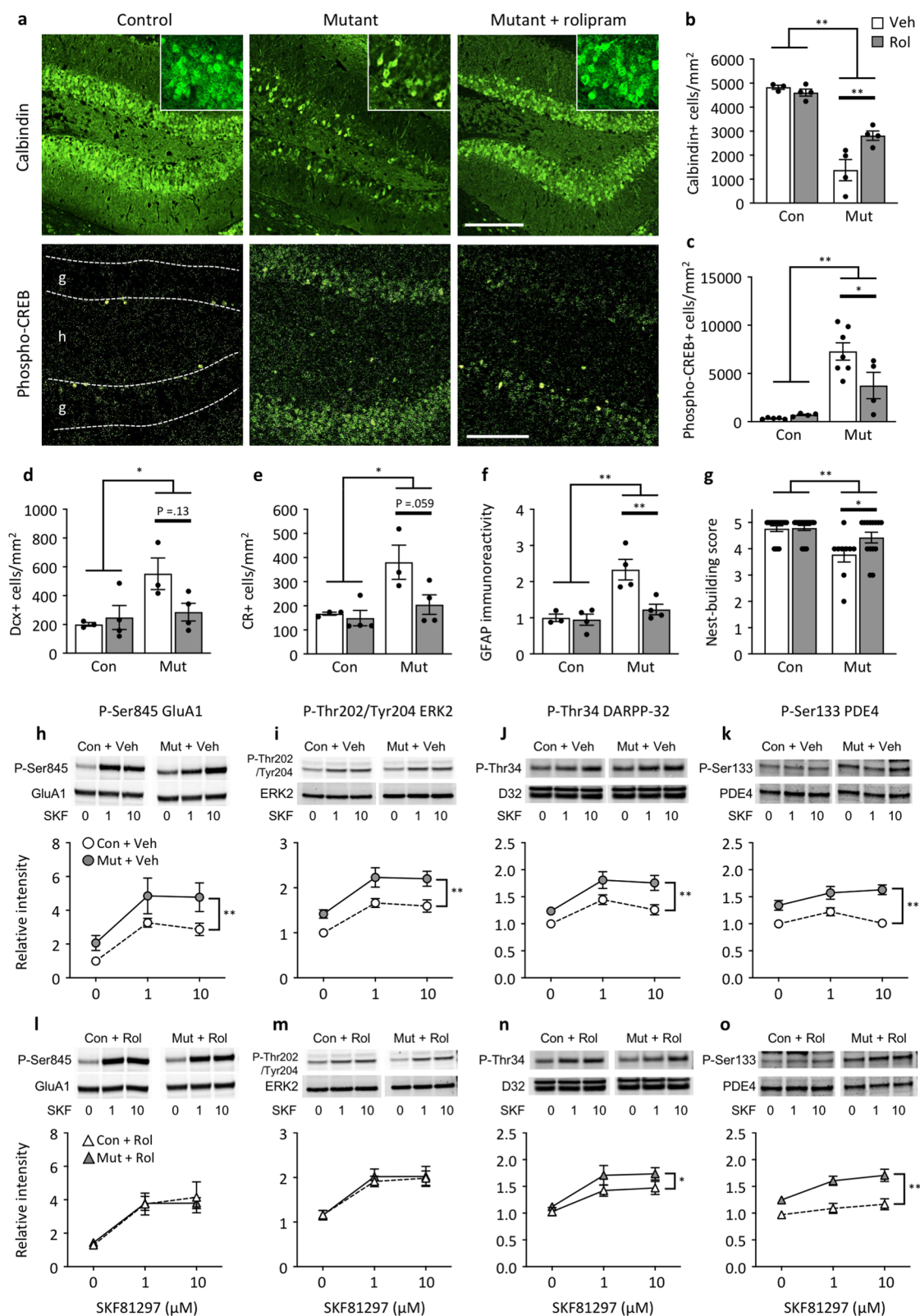


Fig. 4 (See legend on previous page.)

(Additional file 1: Fig. S8). In contrast, in control mice, P-Ser845 GluA1 and P-Thr202/Tyr204 ERK2 levels were shifted upward following chronic rolipram treatment, and the effect of rolipram treatment on P-Thr202/Tyr204 ERK2 levels was significant ($P=0.0070$) (Additional file 1: Fig. S8). These results indicate that chronic rolipram treatment modulates PKA activity downstream of *Drd1a* in a substrate-selective manner with the opposite effect between *Cn* mutant and control mice. When we examined the dose-dependency curves induced by SKF81297 application using data normalized to the level of each group untreated with SKF81297, a similar increase was found in SKF81297-induced phosphorylation between genotypes in ERK2, DARPP-32, and PDE4, but not in GluA1 (Additional file 1: Fig. S9), suggesting that *Drd1* signaling is partially disturbed in *Cn* mutant mice.

Discussion

In this study, we found immaturity-related signatures in the DG of adult *Cn* mutant mice, as assessed by the expression of typical molecular markers for neuronal maturation and genome-wide gene expression patterns. Considering that deletion of the *Cnb1* gene mediated by Cre under the *Camk2a* promoter was not observed until postnatal 5 weeks of age [24], it is likely that the iDG phenotype appears thereafter in the *Cn* mutants. During postnatal mouse development, calbindin expression levels in the DG almost reached a plateau at 4 weeks of age when it did not change further [81]. Therefore, it is likely that *Cn* deficiency starting after 5 weeks of age may reverse the maturity of GCs, designated as dematuration [47]. A number of factors, including genetic [3, 4, 7] and non-genetic factors [5, 47, 82], have been suggested to postnatally induce dematuration of GCs. The iDG phenotype in *Cn* mutants could be another example of dematuration of GCs. The presence of a number of doublecortin- or calretinin-positive immature GCs in the middle and outer parts of the GC layer apart from the subgranular zone (a well-known neurogenic region) is suggested to be attributed to the dematuration of mature GCs rather than to adult neurogenesis [16]. 5-bromo-2'-deoxyuridine (BrdU) labeling assay indicated that adult neurogenesis was slightly but significantly increased in the DG of *Cn* mutants (manuscript in preparation), but no obvious changes were found in the number of GCs. Therefore, enhanced recruitment of new neurons might not be a major contributing factor to the iDG phenotype. However, it is unclear how *Cn* deficiency caused the iDG phenotype in mice, including whether it is mediated by a cell-autonomous or non-cell-autonomous role of *Cn*.

We should note the limitations of the present study. First, while we showed an increase in *Drd1a* expression in the DG of *Cn* mutants by qPCR analysis, it has not

been determined whether the increase appears in GC. Spatial analysis of *Drd1a* expression in combination with specific GC markers using in situ hybridization will help address this issue. Second, pathway enrichment analysis showed that biological processes related to the development of particular cells/tissues were predominantly overrepresented in the DEGs of *Cn* mutants, which is in accordance with the iDG hypothesis in these mice. However, limitations of this analysis include the inequality in annotation between genes in the database used. We queried GO and MsigDB databases via BaseSpace platform. Commonly used databases for pathway analysis, including these, are basically created by the curation of published experimental data. Hence, the analyses using the databases tend to bias toward the already annotated genes in nature, while prior unannotated genes are ignored [83, 84]. Such annotation inequality bias of genes must be taken into consideration to interpret our results of pathway enrichment analysis. Importantly, targeted comparisons revealed the high similarities in the gene expression pattern of *Cn* mutants with that of typically developing infant mice and other established mice with iDG, which confirmed the iDG phenotype in *Cn* mutants in terms of global gene expression analysis, in addition to pathway enrichment analysis.

We found that chronic rolipram treatment rescued the deficits in nest-building behavior along with the iDG phenotype in *Cn* mutants. Nest-building behavior is considered to be a hippocampus-dependent behavior [78–80], and its deficits have been observed in multiple mouse models of neuropsychiatric disorders, including ASD, schizophrenia, and AD [85]. In our previous study, we showed that the rescue of the iDG phenotype was accompanied by the rescue of nesting behavior deficits in *Hivep2* KO mice, a mouse model of schizophrenia and ID [3, 86]. These results suggest that the iDG may be involved in impaired nest-building behavior. However, while we focused on the DG in this study, the effect of *Cnb1* knockout by *Camk2a*-Cre appeared in other areas of the brain, indicating that functional and morphological neuronal abnormalities have been found in the areas, such as synaptic plasticity deficits as assessed by long-term depression [24] and an impaired short-wave ripple-associated replay [87] in the CA1 region of the hippocampus, impaired synaptic transmission induced by high-frequency stimulation and decreased high-frequency oscillatory activity assessed by γ oscillations in the prefrontal cortex [88], and the prevention of spine shrinkage suggested by a reduction in small spines in the prefrontal and visual cortices [27, 28]. In addition, considering that rolipram highly binds to the neocortex, cerebellum, and hippocampus in rodents [89], rolipram may exert its effects in brain areas other than the DG in *Cn*

mutants. The present study did not address the causal link between iDG and impaired nesting behavior. Therefore, we cannot exclude the possibility that impaired nesting behavior is associated with brain abnormalities other than iDG alone or in combination with iDG. It would be of interest to examine whether rolipram treatment rescues the above-mentioned neuronal abnormalities other than iDG.

Under basal conditions, Cn mutants showed increased phosphorylation levels of PKA substrates (PDE4, ERK2, GluA1, DARPP-32, and CREB). P-Ser845 GluA1 is a substrate for Cn [90]. It has also been reported that Cn dephosphorylates P-Thr34 DARPP-32 [91], which inhibits protein phosphatase-1 (PP1) activity [92]. PP1 dephosphorylates GluA1 [93] and CREB [94] directly and indirectly decreases the phosphorylation of ERK2 [95]. Consistent with these observations, we observed that phosphorylation levels of DARPP-32, GluA1, ERK2, and CREB were increased in Cn mutants. In addition to this pathway, increased PKA activity downstream of Drd1 may facilitate CREB phosphorylation in Cn mutants. Phosphorylation of PDE4 at Ser133 increases its activity [96], which is thought to be a negative feedback mechanism that maintains intracellular cAMP levels. Increased Drd1 signaling and PDE4 phosphorylation may balance the production and degradation of cAMP at high levels in Cn mutants. However, CREB, DARPP-32, and ERK are known to be dephosphorylated by protein phosphatase 2A (PP2A) [97–99], which can be activated by PKA through phosphorylation of the B56 δ subunit [100]. Studies are needed to examine activation/expression of PP2A, as well as PP1, to gain further insight into the molecular mechanism underlying the increased basal phosphorylation of these PKA substrates in Cn mutant mice.

The increased Drd1/PKA signaling in Cn mutants relative to that in controls disappeared after chronic rolipram treatment in a PKA substrate-dependent manner. Furthermore, chronic treatment with rolipram ameliorated the increased phosphorylation of CREB, a known PKA substrate. As rolipram is known to increase intracellular cAMP levels and hence activate PKA activity, our data would appear to be paradoxical. These changes are not accounted for by changes in Drd1a expression levels, since rolipram did not significantly affect its expression levels in either Cn mutants or controls. Considering that PKA activates PP2A [100], which is capable of directly dephosphorylating CREB, chronic rolipram administration might facilitate this pathway, resulting in decreased CREB phosphorylation levels in Cn mutants. Interestingly, previous studies have suggested some compensatory mechanisms for constitutive increases and decreases in intracellular cAMP levels by enhancing PDE activity [101] and increasing dopamine concentrations [102].

Based on our data and those of others, we speculate that chronic, sustained upregulation in Drd1a/cAMP/PKA signaling in the Cn mutant DG is a compensatory mechanism underlying the iDG and nesting behavior deficits; thus, facilitating this pathway chronically with rolipram administration might exert beneficial effects, resulting in the rescue of the iDG phenotype and impaired nest-building behavior. However, the exact molecular mechanisms underlying the paradoxical changes in PKA activity in response to rolipram in Cn mutants remain unclear. Other molecules that regulate cAMP levels and PKA activity, such as protein Gs, adenylyl cyclase, PKA regulatory subunit, protein phosphatase, and PDE family members other than PDE4 may be involved in chronic rolipram-related changes in the DG.

While currently available antipsychotic medications are mainly defined by their ability to ameliorate the positive symptoms of schizophrenia, such as delusions and hallucinations, few therapeutic methods have been established for the negative symptoms and cognitive dysfunction of the disease [103–105]. In this study, we found that chronic rolipram treatment rescued the decrease in nest-building activity in Cn mutants. The effect of the drug on the behavior was nominally significant but failed to reach study-wide significance; hence, this finding needs to be replicated in different cohorts. We previously found that rolipram (in combination with ibuprofen) rescued the decreased nest building and iDG phenotype in Hive2 KO mice [3]. Therefore, PDE4 could be considered an important target for the treatment of the phenotypes. Indeed, a pilot study has reported that rolipram treatment exhibited some improvement of symptoms observed in patients with schizophrenia; however, its clinical use is limited due to side effects, such as nausea and vomiting [102], which may be due to the broad action of rolipram on PDE subtypes [106]. The development of PDE4 inhibitors without side effects may be a potential novel treatment for negative symptoms associated with neuronal immaturity in the DG in neuropsychiatric disorders, including schizophrenia [107]. Note that chronic rolipram treatment did not rescue other behavioral abnormalities examined in Cn mutants (e.g., hyperlocomotor activity, impaired PPI, and working memory deficits), suggesting that different molecular bases may underlie each behavioral phenotype.

In conclusion, this study adds to the literature indicating that the iDG phenotype can be induced by many genetic and non-genetic factors and is a possible endophenotype commonly found in neuropsychiatric disorders, including schizophrenia, ID, ASD, epilepsy, and AD [21]. We consider that the iDG in Cn mutants could be a phenotypic model linking Drd1a-mediated hyperdopaminergic dysregulation and neurodevelopmental

abnormalities and may serve as a potential therapeutic target, especially for negative symptoms of neuropsychiatric disorders.

Abbreviations

AD: Alzheimer's disease; ASD: Autism spectrum disorder; Camk2a: Calcium/calmodulin dependent protein kinase II alpha; cAMP: Cyclic adenosine monophosphate; Cn: Calcineurin; CREB: CAMP-dependent response element binding protein; DARPP-32: Dopamine-and cAMP-regulated phosphoprotein of 32 kDa; DEGs: Differentially expressed genes; DG: Dentate gyrus; Drd1: Dopamine D1 receptor; Dsp: Desmoplakin; ERK2: Extracellular signal-regulated kinase 2; GC: Granule cell; GFAP: Glial fibrillary acidic protein; GluA1: Glutamate receptor 1; Hivep2: Human immunodeficiency virus type I enhancer binding protein 2; Iba1: Ionized calcium-binding adaptor molecule 1; ID: Intellectual disability; iDG: Immature dentate gyrus; PDE4: Phosphodiesterase 4; PKA: CAMP/protein kinase A; PSA-NCAM: Polysialylated neural cell adhesion molecule; Tdo2: Tryptophan 2,3-dioxygenase.

Supplementary Information

The online version contains supplementary material available at <https://doi.org/10.1186/s13041-022-00981-0>.

Additional file 1: Supplementary Materials and Methods. **Figure S1.** No significant differences in the expression of mature/immature granule cell markers in the DG among three genotypes used for control mice. **Figure S2.** Decreased expression of GluA1 and GluA2 in the molecular layer of DG in Cn mutant mice. **Figure S3.** Original blots for Fig. 1i. **Figure S4.** Increased expression levels of S100B in the DG of Cn mutant mice. **Figure S5.** No significant effects of chronic rolipram treatment on GluA1 or *Drd1a* expression in the DG of Cn mutant mice. **Figure S6.** No significant effects of chronic rolipram treatment on open field test, PPI, or T-maze spontaneous alteration task in Cn mutant mice. **Figure S7.** Original blots for Fig. 4, S8 and S9. **Figure S8.** Effect of chronic rolipram treatment on phosphorylation levels of PKA substrates in the DG of control and Cn mutant mice. **Figure S9.** Dose-dependent changes in PKA substrate phosphorylation levels by application of SKF81297.

Additional file 2: Table S1. Antibodies used in this study. **Table S2.** Raw data of RT-PCR used for analyses. **Table S3.** Differentially expressed genes (DEGs) in the DG of Cn mutant mice. **Table S4.** Pathway enrichment analysis of DEGs. **Table S5.** Comparison of gene expression patterns in the DG of adult Cn mutant mice with those of infant mice at different time points after birth.

Acknowledgements

We thank Daiki X. Sato for his valuable comments on statistics. We also thank Wakako Hasegawa, Yumiko Mobayashi, Tamaki Murakami, Chikako Ozeki, Yoko Kagami, Harumi Mitsuya, and Yoshihiro Takamiya for their technical assistance. We thank Prof. James A Bibb for providing the P-Ser133 PDE4 antibody.

Author contributions

HH and TM designed experiments. HH and TM wrote the manuscript. HH performed immunohistochemical, gene expression, and bioinformatics analyses. MK and AN performed slice experiments. HS performed behavioral tests. IAG and GRC provided Cn mutant mice. All authors read and approved the final manuscript.

Funding

This work was supported by the Ministry of Education, Culture, Sports, Science and Technology (MEXT KAKENHI Grant Number JP16H06462) and the Japan Society for the Promotion of Science (JSPS KAKENHI Grant Number JP20H00522). The work was supported by grants to GRC from the National Institutes of Health RF1MH126720 and R01CA276167.

Availability of data and materials

The microarray data generated during the current study are available in the GEO database under the accession number GSE175896 (<https://www.ncbi.nlm.nih.gov/geo/>).

Declarations

Ethics approval and consent to participate

Not applicable.

Consent for publication

Not applicable.

Competing interests

The authors declare that they have no competing interests.

Author details

¹Division of Systems Medical Science, Center for Medical Science, Fujita Health University, Toyoake, Aichi 470-1192, Japan. ²Department of Pharmacology, Kurume University School of Medicine, Kurume, Fukuoka 830-0011, Japan. ³Department of Pathology, Stanford University of Medicine, Stanford, CA 94305, USA.

Received: 25 September 2022 Accepted: 12 November 2022

Published online: 22 November 2022

References

- Anderzhanova E, Kirmeier T, Wotjak CT. Animal models in psychiatric research: The RDoC system as a new framework for endophenotype-oriented translational neuroscience. *Neurobiol Stress*. 2017;7:47–56.
- Yamasaki N, Maekawa M, Kobayashi K, Kajii Y, Maeda J, Soma M, et al. Alpha-CaMKII deficiency causes immature dentate gyrus, a novel candidate endophenotype of psychiatric disorders. *Mol Brain*. 2008;1:6.
- Takao K, Kobayashi K, Hagihara H, Ohira K, Shoji H, Hattori S, et al. Deficiency of schnurri-2, an MHC enhancer binding protein, induces mild chronic inflammation in the brain and confers molecular, neuronal, and behavioral phenotypes related to schizophrenia. *Neuropsychopharmacology*. 2013;38:1409–25.
- Ohira K, Kobayashi K, Toyama K, Nakamura HK, Shoji H, Takao K, et al. Synaptosomal-associated protein 25 mutation induces immaturity of the dentate granule cells of adult mice. *Mol Brain*. 2013;6:12.
- Shin R, Kobayashi K, Hagihara H, Kogan JH, Miyake S, Tajinda K, et al. The immature dentate gyrus represents a shared phenotype of mouse models of epilepsy and psychiatric disease. *Bipolar Disord*. 2013;15:405–21.
- Hagihara H, Fujita M, Umemori J, Hashimoto M, Miyakawa T. Immature-like molecular expression patterns in the hippocampus of a mouse model of dementia with Lewy body-linked mutant β -synuclein. *Mol Brain*. 2018;11:38.
- Nagashima S, Ito N, Kobayashi R, Shiiba I, Shimura H, Fukuda T, et al. Forebrain-specific deficiency of the GTPase CRAG/Centaurin- γ 3 leads to immature dentate gyri and hyperactivity in mice. *J Biol Chem*. 2021;296:100620.
- Nakahara S, Miyake S, Tajinda K, Ito H. Mossy fiber mis-pathfinding and semaphorin reduction in the hippocampus of α -CaMKII hKO mice. *Neurosci Lett*. 2015;598:47–51.
- Nakahara S, Adachi M, Ito H, Matsumoto M, Tajinda K, van Erp TGM. Hippocampal pathophysiology: commonality shared by temporal lobe epilepsy and psychiatric disorders. *Neurosci J*. 2018;2018:1–9.
- Palop JJ, Chin J, Roberson ED, Wang J, Thwin MT, Bien-Ly N, et al. Aberrant excitatory neuronal activity and compensatory remodeling of inhibitory hippocampal circuits in mouse models of Alzheimer's disease. *Neuron*. 2007;55:697–711.
- Palop JJ, Jones B, Kekoni L, Chin J, Yu G-Q, Raber J, et al. Neuronal depletion of calcium-dependent proteins in the dentate gyrus is tightly linked to Alzheimer's disease-related cognitive deficits. *Proc Natl Acad Sci*. 2003;100:9572–7.

12. You JC, Muralidharan K, Park JW, Petrof I, Pyfer MS, Corbett BF, et al. Epigenetic suppression of hippocampal calbindin-D28k by Δ FosB drives seizure-related cognitive deficits. *Nat Med.* 2017;23:1377–83.
13. Tavitian A, Song W, Schipper HM. Dentate gyrus immaturity in schizophrenia. *The Neuroscientist.* 2019;1073858418824072.
14. Walton NM, Zhou Y, Kogan JH, Shin R, Webster M, Gross AK, et al. Detection of an immature dentate gyrus feature in human schizophrenia/bipolar patients. *Transl Psychiatry.* 2012;2: e135.
15. Altar CA, Jurata LW, Charles V, Lemire A, Liu P, Bukhman Y, et al. Deficient hippocampal neuron expression of proteasome, ubiquitin, and mitochondrial genes in multiple schizophrenia cohorts. *Biol Psychiatry.* 2005;58:85–96.
16. Hagihara H, Murano T, Ohira K, Miwa M, Nakamura K, Miyakawa T. Expression of progenitor cell/immature neuron markers does not present definitive evidence for adult neurogenesis. *Mol Brain.* 2019;12:108.
17. Murano T, Hagihara H, Tajinda K, Matsumoto M, Miyakawa T. Transcriptomic immaturity inducible by neural hyperexcitation is shared by multiple neuropsychiatric disorders. *Commun Biol.* 2019;2:32.
18. Murano T, Koshimizu H, Hagihara H, Miyakawa T. Transcriptomic immaturity of the hippocampus and prefrontal cortex in patients with alcoholism. *Sci Rep.* 2017;7:44531.
19. Hagihara H, Ohira K, Takao K, Miyakawa T. Transcriptomic evidence for immaturity of the prefrontal cortex in patients with schizophrenia. *Mol Brain.* 2014;7:41.
20. Gandal MJ, Nesbitt AM, McCurdy RM, Alter MD. Measuring the maturity of the fast-spiking interneuron transcriptional program in autism, schizophrenia, and bipolar disorder. *PLoS ONE.* 2012;7: e41215.
21. Hagihara H, Takao K, Walton NM, Matsumoto M, Miyakawa T. Immature dentate gyrus: an endophenotype of neuropsychiatric disorders. *Neural Plast.* 2013;2013:1.
22. Rusnak F, Mertz P. Calcineurin: form and function. *Physiol Rev.* 2000;80:1483–521.
23. Takaishi T, Saito N, Kuno T, Tanaka C. Differential distribution of the mRNA encoding two isoforms of the catalytic subunit of calcineurin in the rat brain. *Biochem Biophys Res Commun.* 1991;174:393–8.
24. Zeng H, Chattarji S, Barbarosie M, Rondi-Reig L, Philpot BD, Miyakawa T, et al. Forebrain-specific calcineurin knockout selectively impairs bidirectional synaptic plasticity and working/episodic-like memory. *Cell.* 2001;107:617–29.
25. Mulkey RM, Endo S, Shenolikar S, Malenka RC. Involvement of a calcineurin/ inhibitor-1 phosphatase cascade in hippocampal long-term depression. *Nature.* 1994;369:486–8.
26. Li S-T, Kato K, Tomizawa K, Matsushita M, Moriwaki A, Matsui H, et al. Calcineurin plays different roles in group II metabotropic glutamate receptor- and NMDA receptor-dependent long-term depression. *J Neurosci.* 2002;22:5034–41.
27. Okazaki H, Hayashi-Takagi A, Nagaoka A, Negishi M, Ucar H, Yagishita S, et al. Calcineurin knockout mice show a selective loss of small spines. *Neurosci Lett.* 2018;671:99–102.
28. Kasai H, Ziv NE, Okazaki H, Yagishita S, Toyozumi T. Spine dynamics in the brain, mental disorders and artificial neural networks. *Nat Rev Neurosci.* 2021;22:407–22.
29. Wen Z, Guirland C, Ming G, Zheng JQ. A CaMKII/calcineurin switch controls the direction of Ca²⁺-dependent growth cone guidance. *Neuron.* 2004;43:835–46.
30. Graef IA, Wang F, Charron F, Chen L, Neilson J, Tessier-Lavigne M, et al. Neurotrophins and netrins require calcineurin/NFAT signaling to stimulate outgrowth of embryonic axons. *Cell.* 2003;113:657–70.
31. Gerber DJ, Hall D, Miyakawa T, Demars S, Gogos JA, Karayiorgou M, et al. Evidence for association of schizophrenia with genetic variation in the 8p21.3 gene, PPP3CC, encoding the calcineurin gamma subunit. *Proc Natl Acad Sci.* 2003;100:8993–8.
32. Liu YL, Fann CSJ, Liu CM, Chang CC, Yang WC, Hung SI, et al. More evidence supports the association of PPP3CC with schizophrenia. *Mol Psychiatry.* 2007;12:966–74.
33. Horiuchi Y, Ishiguro H, Koga M, Inada T, Iwata N, Ozaki N, et al. Support for association of the PPP3CC gene with schizophrenia. *Mol Psychiatry.* 2007;12:891–3.
34. Yamada K, Gerber DJ, Iwayama Y, Ohnishi T, Ohba H, Toyota T, et al. Genetic analysis of the calcineurin pathway identifies members of the EGR gene family, specifically EGR3, as potential susceptibility candidates in schizophrenia. *Proc Natl Acad Sci.* 2007;104:2815–20.
35. Rydzanicz M, Wachowska M, Cook EC, Lisowski P, Kuźniewska B, Szymańska K, et al. Novel calcineurin A (PPP3CA) variant associated with epilepsy, constitutive enzyme activation and downregulation of protein expression. *Eur J Hum Genet.* 2019;27:61–9.
36. Myers CT, Stong N, Moutier EI, Helbig KL, Freytag S, Sullivan JE, et al. De novo mutations in PPP3CA cause severe neurodevelopmental disease with seizures. *Am J Hum Genet.* 2017;101:516–24.
37. Qian Y, Wu B, Lu Y, Dong X, Qin Q, Zhou W, et al. Early-onset infant epileptic encephalopathy associated with a de novo PPP3CA gene mutation. *Mol Case Stud.* 2018;4: a002949.
38. Panneerselvam S, Wang J, Zhu W, Dai H, Pappas JG, Rabin R, et al. PPP3CA truncating variants clustered in the regulatory domain cause early-onset refractory epilepsy. *Clin Genet.* 2021;100:227–33.
39. Mizuguchi T, Nakashima M, Kato M, Okamoto N, Kurahashi H, Ekhlévitch N, et al. Loss-of-function and gain-of-function mutations in PPP3CA cause two distinct disorders. *Hum Mol Genet.* 2018;27:1421–33.
40. Li J, Gao K, Yan H, Xiangwei W, Liu N, Wang T, et al. Reanalysis of whole exome sequencing data in patients with epilepsy and intellectual disability/mental retardation. *Gene.* 2019;700:168–75.
41. Singh T, Poterba T, Curtis D, Akil H, Al Eissa M, Barchas JD, et al. Rare coding variants in ten genes confer substantial risk for schizophrenia. *Nature.* 2022;604:509–16.
42. Trubetskoy V, Pardiñas AF, Qi T, Panagiotaropoulou G, Awasthi S, Bigdeli TB, et al. Mapping genomic loci implicates genes and synaptic biology in schizophrenia. *Nature.* 2022;604:502–8.
43. Zinkstok JR, Boot E, Bassett AS, Hiroi N, Butcher NJ, Vingerhoets C, et al. Neurobiological perspective of 22q11.2 deletion syndrome. *Lancet Psychiatry.* 2019;6:951–60.
44. Voineagu I, Wang X, Johnston P, Lowe JK, Tian Y, Horvath S, et al. Transcriptomic analysis of autistic brain reveals convergent molecular pathology. *Nature.* 2011;474:380–4.
45. Pedersen CS, Sørensen DB, Parachikova AI, Plath N. PCP-induced deficits in murine nest building activity: employment of an ethological rodent behavior to mimic negative-like symptoms of schizophrenia. *Behav Brain Res.* 2014;273:63–72.
46. Miyakawa T, Leiter LM, Gerber DJ, Gainetdinov RR, Sotnikova TD, Zeng H, et al. Conditional calcineurin knockout mice exhibit multiple abnormal behaviors related to schizophrenia. *Proc Natl Acad Sci.* 2003;100:8987–92.
47. Kobayashi K, Ikeda Y, Sakai A, Yamasaki N, Haneda E, Miyakawa T, et al. Reversal of hippocampal neuronal maturation by serotonergic antidepressants. *Proc Natl Acad Sci.* 2010;107:8434–9.
48. Shuto T, Kuroiwa M, Sotogaku N, Kawahara Y, Oh Y-S, Jang J-H, et al. Obligatory roles of dopamine D1 receptors in the dentate gyrus in antidepressant actions of a selective serotonin reuptake inhibitor, fluoxetine. *Mol Psychiatry.* 2018;25:1229–44.
49. Abi-Dargham A. Recent evidence for dopamine abnormalities in schizophrenia. *Eur Psychiatry.* 2002;17:341s–7s.
50. Abi-Dargham A, Mawlawi O, Lombardo I, Gil R, Martinez D, Huang Y, et al. Prefrontal dopamine D1 receptors and working memory in schizophrenia. *J Neurosci.* 2002;22:3708–19.
51. Cervenka S. PET radioligands for the dopamine D1-receptor: application in psychiatric disorders. *Neurosci Lett.* 2019;691:26–34.
52. Neilson JR, Winslow MM, Hur EM, Crabtree GR. Calcineurin B1 is essential for positive but not negative selection during thymocyte development. *Immunity.* 2004;20:255–66.
53. Tsien JZ, Chen DF, Gerber D, Tom C, Mercer EH, Anderson DJ, et al. Subregion- and cell type-restricted gene knockout in mouse brain. *Cell.* 1996;87:1317–26.
54. Hagihara H, Horikawa T, Nakamura HK, Umemori J, Shoji H, Kamitani Y, et al. Circadian gene circuitry predicts hyperactive behavior in a mood disorder mouse model. *Cell Rep.* 2016;14:2784–96.
55. Hagihara H, Shoji H, Otabi H, Toyoda A, Katoh K, Namihira M, et al. Protein lactylation induced by neural excitation. *Cell Rep.* 2021;37:109820.
56. Franklin KBJ, Paxinos G. The mouse brain in stereotaxic coordinates. San Diego: Academic Press Inc.; 1997.

57. Hagihara H, Toyama K, Yamasaki N, Miyakawa T. Dissection of hippocampal dentate gyrus from adult mouse. *J Vis Exp JoVE*. 2009. <https://doi.org/10.3791/1543>.
58. Hagihara H, Ohira K, Miyakawa T. Transcriptomic evidence for immaturity induced by antidepressant fluoxetine in the hippocampus and prefrontal cortex. *Neuropsychopharmacol Rep*. 2019;39:78–89.
59. Kupersmidt I, Su QJ, Grewal A, Sundaresh S, Halperin I, Flynn J, et al. Ontology-based meta-analysis of global collections of high-throughput public data. *PLoS ONE*. 2010;5: e13066.
60. Nakajima R, Hagihara H, Miyakawa T. Similarities of developmental gene expression changes in the brain between human and experimental animals: rhesus monkey, mouse, zebrafish, and drosophila. *Mol Brain*. 2021;14:135.
61. Takao K, Miyakawa T. Genomic responses in mouse models greatly mimic human inflammatory diseases. *Proc Natl Acad Sci U S A*. 2015;112:1167–72.
62. Nakajima R, Takao K, Hattori S, Shoji H, Komiyama NH, Grant SGN, et al. Comprehensive behavioral analysis of heterozygous Syngap1 knockout mice. *Neuropsychopharmacol Rep*. 2019;39:223–37.
63. Hattori S, Okumura Y, Takao K, Yamaguchi Y, Miyakawa T. Open source code for behavior analysis in rodents. *Neuropsychopharmacol Rep*. 2019;39:67–9.
64. Deacon RM. Assessing nest building in mice. *Nat Protoc*. 2006;1:1117–9.
65. Hagihara H, Ohira K, Toyama K, Miyakawa T. Expression of the AMPA receptor subunits GluR1 and GluR2 is associated with granule cell maturation in the dentate gyrus. *Front Neurosci*. 2011;5:100.
66. Ohira K, Hagihara H, Toyama K, Takao K, Kanai M, Funakoshi H, et al. Expression of tryptophan 2,3-dioxygenase in mature granule cells of the adult mouse dentate gyrus. *Mol Brain*. 2010;3:26.
67. Bender RA, Lauterborn JC, Gall CM, Cariaga W, Baram TZ. Enhanced CREB phosphorylation in immature dentate gyrus granule cells precedes neurotrophin expression and indicates a specific role of CREB in granule cell differentiation. *Eur J Neurosci*. 2001;13:679–86.
68. Hwang IK, Yoo K-Y, Yoo DY, Choi JW, Lee CH, Choi JH, et al. Time-course of changes in phosphorylated CREB in neuroblasts and BDNF in the mouse dentate gyrus at early postnatal stages. *Cell Mol Neurobiol*. 2011;31:669.
69. Merz K, Herold S, Lie DC. CREB in adult neurogenesis—master and partner in the development of adult-born neurons? *Eur J Neurosci*. 2011;33:1078–86.
70. Vargas DL, Nascimbene C, Krishnan C, Zimmerman AW, Pardo CA. Neuroglial activation and neuroinflammation in the brain of patients with autism. *Ann Neurol*. 2005;57:67–81.
71. Menassa DA, Sloan C, Chance SA. Primary olfactory cortex in autism and epilepsy: increased glial cells in autism. *Brain Pathol*. 2017;27:437–48.
72. Griffin WST, Sheng JG, McKenzie JE, Royston MC, Gentleman SM, Brumback RA, et al. Life-long overexpression of S100 β in Down's syndrome: implications for Alzheimer pathogenesis. *Neurobiol Aging*. 1998;19:401–5.
73. Crespel A, Coubes P, Rousset M-C, Brana C, Rougier A, Rondouin G, et al. Inflammatory reactions in human medial temporal lobe epilepsy with hippocampal sclerosis. *Brain Res*. 2002;952:159–69.
74. Johnson AM, Sugo E, Barreto D, Hiew C-C, Lawson JA, Connolly AM, et al. The severity of gliosis in hippocampal sclerosis correlates with pre-operative seizure burden and outcome after temporal lobectomy. *Mol Neurobiol*. 2016;53:5446–56.
75. Catts VS, Wong J, Fillman SG, Fung SJ, Weickert CS. Increased expression of astrocyte markers in schizophrenia: association with neuroinflammation. *Aust N Z J Psychiatry*. 2014;48:722–34.
76. Toker L, Mancarci BO, Tripathy S, Pavlidis P. Transcriptomic evidence for alterations in astrocytes and parvalbumin interneurons in subjects with bipolar disorder and schizophrenia. *Biol Psychiatry*. 2018;84:787–96.
77. Verkhatsky A, Rodrigues JJ, Pivoriunas A, Zorec R, Semyanov A. Astroglial atrophy in Alzheimer's disease. *Pflug Arch Eur J Physiol*. 2019;471:1247–61.
78. Kandel ER. The molecular biology of memory: cAMP, PKA, CRE, CREB-1, CREB-2, and CPEB. *Mol Brain*. 2012;5:14.
79. Heit JJ. Calcineurin/NFAT signaling in the β -cell: from diabetes to new therapeutics. *BioEssays*. 2007;29:1011–21.
80. Zhu J, Mix E, Winblad B. The antidepressant and antiinflammatory effects of rolipram in the central nervous system. *CNS Drug Rev*. 2001;7:387–98.
81. Radic T, Frieß L, Vijikumar A, Jungenitz T, Deller T, Schwarzacher SW. Differential postnatal expression of neuronal maturation markers in the dentate gyrus of mice and rats. *Front Neuroanat*. 2017;11.
82. Imoto Y, Segi-Nishida E, Suzuki H, Kobayashi K. Rapid and stable changes in maturation-related phenotypes of the adult hippocampal neurons by electroconvulsive treatment. *Mol Brain*. 2017;10:8.
83. Haynes WA, Tomczak A, Khatri P. Gene annotation bias impedes biomedical research. *Sci Rep*. 2018;8:1362.
84. Timmons JA, Szkop KJ, Gallagher JJ. Multiple sources of bias confound functional enrichment analysis of global -omics data. *Genome Biol*. 2015;16:186.
85. Jirkof P. Burrowing and nest building behavior as indicators of well-being in mice. *J Neurosci Methods*. 2014;234:139–46.
86. Nakao A, Miyazaki N, Ohira K, Hagihara H, Takagi T, Usuda N, et al. Immature morphological properties in subcellular-scale structures in the dentate gyrus of Schnurri-2 knockout mice: a model for schizophrenia and intellectual disability. *Mol Brain*. 2017;10:60.
87. Suh J, Foster DJ, Davoudi H, Wilson MA, Tonegawa S. Impaired hippocampal ripple-associated replay in a mouse model of schizophrenia. *Neuron*. 2013;80:484–93.
88. Cottrell JR, Levenson JM, Kim SH, Gibson HE, Richardson KA, Sivula M, et al. Working memory impairment in calcineurin knock-out mice is associated with alterations in synaptic vesicle cycling and disruption of high-frequency synaptic and network activity in prefrontal cortex. *J Neurosci*. 2013;33:10938–49.
89. Kato H, Araki T, Chen T, Itoyama Y, Kogure K. Effect of rolipram on age-related changes in cyclic AMP-selective phosphodiesterase in the rat brain: an autoradiographic study. *Methods Find Exp Clin Pharmacol*. 1998;20:403.
90. Snyder GL, Galdi S, Fienberg AA, Allen P, Nairn AC, Greengard P. Regulation of AMPA receptor dephosphorylation by glutamate receptor agonists. *Neuropharmacology*. 2003;45:703–13.
91. Nishi A, Bibb JA, Matsuyama S, Hamada M, Higashi H, Nairn AC, et al. Regulation of DARPP-32 dephosphorylation at PKA- and Cdk5-sites by NMDA and AMPA receptors: distinct roles of calcineurin and protein phosphatase-2A. *J Neurochem*. 2002;81:832–41.
92. Nishi A, Snyder GL, Greengard P. Bidirectional regulation of DARPP-32 phosphorylation by dopamine. *J Neurosci*. 1997;17:8147–55.
93. Snyder GL, Allen PB, Fienberg AA, Valle CG, Hagan RL, Nairn AC, et al. Regulation of phosphorylation of the GluR1 AMPA receptor in the neostriatum by dopamine and psychostimulants in vivo. *J Neurosci*. 2000;20:4480–8.
94. Alberts AS, Montminy M, Shenolikar S, Feramisco JR. Expression of a peptide inhibitor of protein phosphatase 1 increases phosphorylation and activity of CREB in NIH 3T3 fibroblasts. *Mol Cell Biol*. 1994;14:4398–407.
95. Valjent E, Pascoli V, Svenningsson P, Paul S, Enslin H, Corvol J-C, et al. Regulation of a protein phosphatase cascade allows convergent dopamine and glutamate signals to activate ERK in the striatum. *Proc Natl Acad Sci U S A*. 2005;102:491–6.
96. Kuroiwa M, Snyder GL, Shuto T, Fukuda A, Yanagawa Y, Benavides DR, et al. Phosphodiesterase 4 inhibition enhances the dopamine D1 receptor/PKA/DARPP-32 signaling cascade in frontal cortex. *Psychopharmacology*. 2012;219:1065–79.
97. Wadzinski BE, Wheat WH, Jaspers S, Peruski LF, Lickeig RL, Johnson GL, et al. Nuclear protein phosphatase 2A dephosphorylates protein kinase A-phosphorylated CREB and regulates CREB transcriptional stimulation. *Mol Cell Biol*. 1993;13:2822–34.
98. Svenningsson P, Nishi A, Fisone G, Girault J-A, Nairn AC, Greengard P. DARPP-32: an integrator of neurotransmission. *Annu Rev Pharmacol Toxicol*. 2004;44:269–96.
99. Letourneux C, Rocher G, Porteu F. B56-containing PP2A dephosphorylate ERK and their activity is controlled by the early gene IEX-1 and ERK. *EMBO J*. 2006;25:727–38.
100. Ahn J-H, McAvoy T, Rakhilin SV, Nishi A, Greengard P, Nairn AC. Protein kinase A activates protein phosphatase 2A by phosphorylation of the B56delta subunit. *Proc Natl Acad Sci U S A*. 2007;104:2979–84.

101. Kelly MP, Isiegas C, Cheung Y-F, Tokarczyk J, Yang X, Esposito MF, et al. Constitutive activation of Gas within forebrain neurons causes deficits in sensorimotor gating because of PKA-dependent decreases in cAMP. *Neuropsychopharmacology*. 2007;32:577–88.
102. Siuciak JA, McCarthy SA, Chapin DS, Martin AN. Behavioral and neurochemical characterization of mice deficient in the phosphodiesterase-4B (PDE4B) enzyme. *Psychopharmacology*. 2008;197:115–26.
103. Davis MC, Horan WP, Marder SR. Psychopharmacology of the negative symptoms: current status and prospects for progress. *Eur Neuropsychopharmacol*. 2014;24:788–99.
104. Fusar-Poli P, Papanastasiou E, Stahl D, Rocchetti M, Carpenter W, Shergill S, et al. Treatments of negative symptoms in schizophrenia: meta-analysis of 168 randomized placebo-controlled trials. *Schizophr Bull*. 2015;41:892–9.
105. Velthorst E, Koeter M, van der Gaag M, Nieman DH, Fett A-KJ, Smit F, et al. Adapted cognitive-behavioural therapy required for targeting negative symptoms in schizophrenia: meta-analysis and meta-regression. *Psychol Med*. 2015;45:453–65.
106. Wang P, Wu P, Ohleth KM, Egan RW, Billah MM. Phosphodiesterase 4B2 is the predominant phosphodiesterase species and undergoes differential regulation of gene expression in human monocytes and neutrophils. *Mol Pharmacol*. 1999;56:170–4.
107. Houslay MD, Schafer P, Zhang KYJ. Keynote review: phosphodiesterase-4 as a therapeutic target. *Drug Discov Today*. 2005;10:1503–19.

Publisher's Note

Springer Nature remains neutral with regard to jurisdictional claims in published maps and institutional affiliations.

Ready to submit your research? Choose BMC and benefit from:

- fast, convenient online submission
- thorough peer review by experienced researchers in your field
- rapid publication on acceptance
- support for research data, including large and complex data types
- gold Open Access which fosters wider collaboration and increased citations
- maximum visibility for your research: over 100M website views per year

At BMC, research is always in progress.

Learn more biomedcentral.com/submissions

